ARTICLE

# $N_2O$ Decomposition over K-Ce Promoted Co-M-Al Mixed Oxide Catalysts Prepared from Hydrotalcite-like Precursors

Jin-li Zhang[a], Shuang Wu[a], Hui Hu[a*], Gao-ming Wu[b*], Zhao-wei Zeng[a]

*a. School of Environmental Science and Engineering, Huazhong University of Science and Technology, Wuhan 430074, China*
*b. Wuhan Iron and Steel (Group) Corp., Wuhan 430083, China*

(Dated: Received on October 29, 2013; Accepted on December 26, 2013)

A series of mixed oxide catalysts with different composition of Co-M-Al and Co-M-Ce-Al (M=Zn, Ni, Cu) were prepared by co-precipitation method from hydrotalcite-like compounds. The experimental results revealed the catalytic activity of Co-Ni-Al is slightly higher than that of Co-Zn-Al and much higher than that of Co-Cu-Al for direct decomposition of $N_2O$. Moreover, addition of small amounts of $CeO_2$ improved the catalytic activity significantly and made the decomposition temperatures at which the $N_2O$ conversion was 50% and 90% ($T_{50}$ and $T_{90}$) both decreased 80 °C than those of Co-M-Al catalysts without $CeO_2$ added. Further, potassium-load also promoted the catalytic activity, and the decomposition temperatures of $T_{50}$ and $T_{90}$ both decreased approximately 50 °C. It is significant for decomposing $N_2O$ from industries and reducing carbon emission from atmosphere.

**Key words:** $N_2O$, Catalytic decomposition, Hydrotalcite-like compound, $CeO_2$, Alkali metal

## I. INTRODUCTION

Nitrous oxide ($N_2O$), as one of the major greenhouse gases in Kyoto Protocol and also as the gas depleting the ozone layer, has a global warming potential (GWP) of 310 and longer atmospheric residence time (120 years). Therefore, $N_2O$ abatement has received more and more attentions recently [1]. However, $N_2O$ concentration has risen continuously by 0.2%−0.3% per year [2], which emits from both natural and anthropogenic sources such as coal combustion, nitric acid plants, adipic acid plants and fluidized bed combustors [3−6]. Direct catalytic decomposition is considered as a perfect method because it can decompose directly $N_2O$ to $N_2$ and $O_2$ without accretion and the process is without secondary pollution. Various types of catalysts have been reported to decompose $N_2O$ [7−11].

In recent years, mixed oxides derived from hydrotalcite-like compounds (HTLCs) as new catalysts exhibited high catalytic activity in decomposing $N_2O$ to $N_2$ and $O_2$ [12], and transition metals such as Co [13], Ni [14], and Zn [15] were used respectively to replace Mg of hydrotalcite-like compounds and showed better decomposition activity. Karásková *et al.* revealed alkali metal potassium in Co-Mn-Al mixed oxide as a promoter to improve catalytic activity for $N_2O$ catalytic decomposition [16]. Xue *et al.* found the addition of $CeO_2$ to the cobalt spinel led to an enhanced catalytic activity for the direct decomposition of $N_2O$ [17]. Hu *et al.* investigated the effect of $SO_2$ reduction over $CeO_2$-$La_2O_3/\gamma$-$Al_2O_3$ and also showed the rare earth metal Ce could accelerate the transfer of surface O and eventually improve catalytic activity [18]. However, the effect of rare earth metal Ce on hydrotalcite-like compounds for $N_2O$ decomposition was rarely investigated, and there were no reports about the synergistic effect of three aspects of transition metal, rare-earth metal, and alkali metal on hydrotalcite-like compounds for direct decomposition of $N_2O$.

In this work, catalysts Co-M-Al and Co-M-Ce-Al (M=Zn, Ni, Cu) with different compositions were prepared by co-precipitation method, and then Co-M-Ce-Al (M=Zn, Ni) mixed oxide catalysts as the carriers of the catalysts to be loaded potassium oxide by impreasgnation method, finally were tested for the catalytic decomposition of $N_2O$. X-ray powder diffraction (XRD), Fourier-transform infrared absorption spectra (FTIR) and X-ray photoelectron spectroscopy (XPS) methods were used to characterize the catalysts.

## II. EXPERIMENTS

### A. Catalyst preparation and characterization

The catalysts of Co-M-Al and Co-M-Ce-Al (M=Zn, Ni, Cu) were prepared by the co-precipitation method. The precursor salts were metal nitrates including

*Authors to whom correspondence should be addressed. E-mail: zjlzjl@hust.edu.cn, gm_wu1031@163.com, Tel.: +86-27-87542224, FAX: +86-27-87792101

 

$Co(NO_3)_2{\cdot}6H_2O$, $Zn(NO_3)_2{\cdot}6H_2O$, $Ni(NO_3)_2{\cdot}6H_2O$, $Cu(NO_3)_2{\cdot}2H_2O$, and $(NO_3)_3{\cdot}9H_2O$ (Sinopharm Chemical Reagent Co., Ltd., A.C.S. grade). $Co_xM_{3-x}$Al-HTLC ($x$=0, 0.5, 1, 1.5, 2, 2.5, or 3, where $x$ is the Co/M molar ratio) was added to the NaOH-$Na_2CO_3$ solution drop wise under stirring at 40 °C and the pH was controlled to 10. The precipitate slurry was stirred for 1 h and heated at 65 °C for 24 h. The resulting products were separated and washed with distilled water until the pH reached 7, and then being dried at 100 °C for 18 h. These $Co_xM_{3-x}$-$Ce_y$-Al-HTLCs samples with different composition were also prepared using the above method and designated as $Co_xM_{3-x}$-$Ce_y$-Al-HTLC, where $y$ is expressed as the molar ratio of Ce/(Co+M). Co-M-Al-HTLC and Co-M-Ce-Al-HTLC samples were calcined at 500 °C to form Co-M-Al and Co-M-Ce-Al mixed oxide catalysts.

Supported catalyst Co-M-Ce-Al (M=Zn or Ni) was prepared by co-precipitation method as above and then impregnated into $K_2CO_3$ (Sinopharm Chemical Reagent Co., Ltd, A.C.S. grade) solution. The mixed liquid was treated for 1 h in ultrasonic generator and then dried in a vacuum oven at 100 °C for 18 h, finally crushed and calcined at 500 °C for 1 h in a muffle furnace. The prepared catalysts were thus referred as $z$K/$Co_xM_{3-x}$-$Ce_y$ ($z$ indicates the loading in mass ratio of $K_2O$, and $z$=0%, 0.5%, 1%, 1.5%, 2%).

The samples were characterized by X-ray diffraction (XRD, PANalytical, Netherlands, Cu K$\alpha$ radiation, and 1.5418 nm) to check the crystal structure of catalysts with a $2\theta$ range of 5°−70° in 0.01°/step. FTIR were recorded using the KBr pellet technique on the spectrometer FTIR (VERTEX 70, Germany) in the range 4000−400 $cm^{-1}$ and the resolution of 4 $cm^{-1}$. The catalysts were analyzed using XPS (Vacuum Generators, UK, Al K$\alpha$ radiation, 1486.6 eV) to identify the surface nature and concentration of the active species with a constant pass energy of 50 eV and charging effects were corrected by referencing C1s measurements at 284.6 eV.

### B. Catalytic activity test

The catalytic reaction was carried out in a fixed-bed quartz flow reactor ($\varphi$=8 mm), containing approximately 1.0 g of catalyst in all the experiments. The reactor was heated by a temperature controlled furnace with a thermocouple. The testing system consisted of of $N_2$, flowmeter, mixed gas chamber, reactor and gas chromatograph. Before the experiment, all samples were pretreated for 30 min in air at 500 °C, and then decreased to the reaction temperature. Finally reaction mixture of $N_2O$ (4000 ppm) in $N_2$ was introduced into the reactor at a flow rate of 400 mL and the space velocity (W/F) was approximately 24000 $h^{-1}$. For reliable $N_2O$ conversion rate, the reaction system was kept for 1 h at each reaction temperature to reach steady state and the reaction products were analyzed in off-gases with a gas chromatographs (Agilent 6890A) equipped with HP-PLOT/Q capillary columns (30 m×0.32 mm×20 μm) and ECD detector, respectively. In all tests, $N_2$ and $O_2$ were the only gaseous products we observed. The temperature range was from 200 °C to 650 °C, and the effect of catalytic activity was expressed by the conversion rate of $N_2O$. The conversion of reactant $X$ was calculated using Eq.(1).

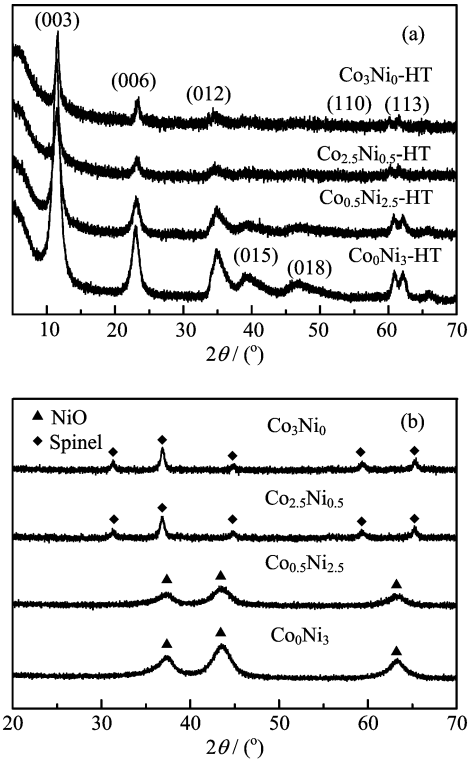


FIG. 1 XRD patterns of (a) Co-Ni-Al-HTLCs and (b) Co-Ni-Al mixed oxides.

$$X(N_2O) = \frac{C_{in}(N_2O) - C_{out}(N_2O)}{C_{in}(N_2O)} \times 100\% \qquad (1)$$

where $X(N_2O)$ is conversion rate of $N_2O$, $C_{in}(N_2O)$ and $C_{out}(N_2O)$ are concentrations of $N_2O$ (ppm) in inlet and outlet, respectively.

## III. RESULTS AND DISCUSSION

### A. Structural characteristics of Co-M-Al-HTLCs and catalytic activity of derived Co-M-Al mixed oxides

In this work, all Co-M-Al-HTLCs and Co-M-Al mixed oxides were characterized by XRD. The XRD spectra of Co-Ni-Al-HTLCs and Co-Ni-Al mixed oxides are shown in Fig.1. From Fig.1(a), the crystallographic indices in XRD patterns of fresh Co-M-Al-HTLCs such as (003), (006), (110), and (113) diffraction lines exhibited the crystal characteristics of hydrotalcite-like

DOI:10.1063/1674-0068/27/02/233-239 

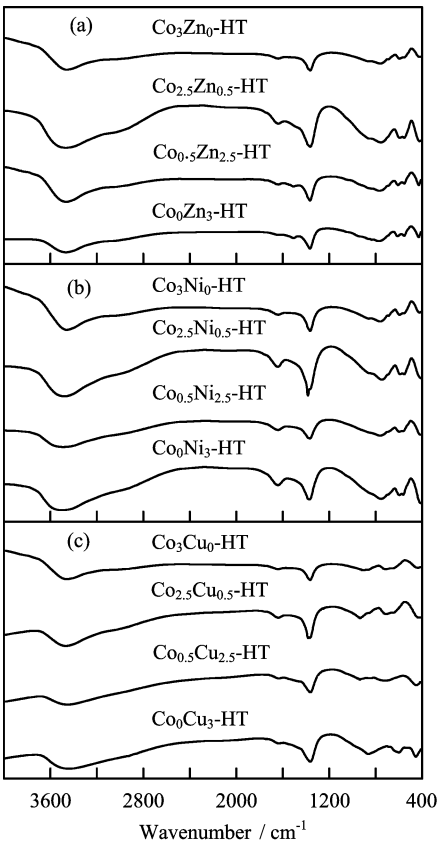


FIG. 2 FTIR spectra of (a) Co-Zn-Al-HTLCs, (b) Co-Ni-Al-HTLCs, and (c) Co-Cu-Al-HTLCs.

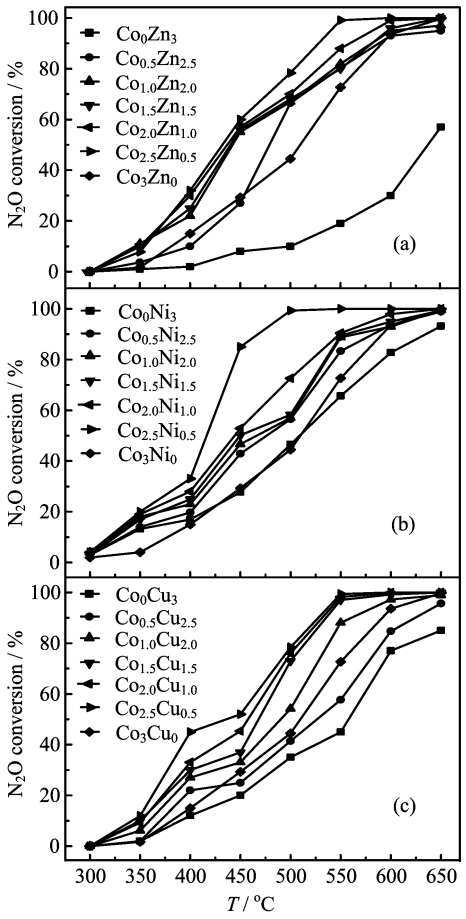


FIG. 3 Conversion of $N_2O$ as a function of reaction temperature over (a) Co-Zn-Al, (b) Co-Ni-Al, and (c) Co-Cu-Al mixed oxides. Reaction conditions: 4000 ppm $N_2O$, $N_2$ balance, GHSV=24000 $h^{-1}$.

materials, it indicated all Co-Ni-Al-HTLCs samples formed the hydrotalcite characteristic diffraction peak [19]. XRD patterns of the calcined Co-Ni-Al-HTLCs are shown in Fig.1(b). The main crystal phase of $Co_0Ni_3$ and $Co_{0.5}Ni_{2.5}$ was NiO, but the main crystal phase of $Co_{2.5}Ni_{0.5}$ and $Co_3Ni_0$ was spinel phase. It was seen that the characteristic diffraction peaks of HTLCs disappeared, indicating the complete collapse of double layered structure after being calcined at 500 °C. Compared with $Co_{2.5}Ni_{0.5}$ and $Co_{0.5}Ni_{2.5}$, we found that spinel type diffraction peak became increasingly sharp with the Co content increasing, and the peak intensity increased, finally the crystallinity became better. Moreover, the segregation phenomenon of NiO decreased gradually and the NiO diffraction peak became more dispersed.

It can be seen from Fig.2 the FTIR spectra of all the Co-M-Al-HTLCs samples also exhibited some characteristics of hydrotalcite-like materials. The broad band around 3450 $cm^{-1}$ was ascribed to the stretching mode of hydroxyl groups. The intense band at 1380 $cm^{-1}$ was due to the asymmetric stretching mode of C=O in $CO_3{}^{2-}$ and shifted to lower frequency in contrast to that in $CaCO_3$, indicating the strong hydrogen bonding of water molecules with interlayer carbonate anions. The band below 800 $cm^{-1}$ was the skeletal vibration of metal-O bonds and hydrotalcite-like [20].

The $N_2O$ conversions over Co-M-Al mixed oxides with different compositions are shown in Fig.3. Compared with $Co_0M_3Al$, it could be seen that the partial replacement of $M^{2+}$ (M=Zn, Ni, Cu) by $Co^{2+}$ with different degree led to a significant improvement in the catalytic activity for the $N_2O$ decomposition. With the increasing of Co content ($0<x<3$), the catalytic activity was improved gradually. Especially among Co-M-Al mixed oxide catalysts, the group with $Co_{2.5}M_{0.5}$ exhibited the best catalytic activity. A further increase in $Co^{2+}$ content caused a decrease in the $N_2O$ decomposition activity.

### B. Impact of Ce on catalytic activity of Co-M-Al samples

Figure 4 revealed the catalytic activity of $N_2O$ over Co-M-Ce-Al mixed oxides. It can be seen that the mixed Ce in catalyst Co-M-Al gave rise to an increase of the catalytic activity and the activity decreased with increasing of the Ce amount. When the molar ratio of

DOI:10.1063/1674-0068/27/02/233-239 

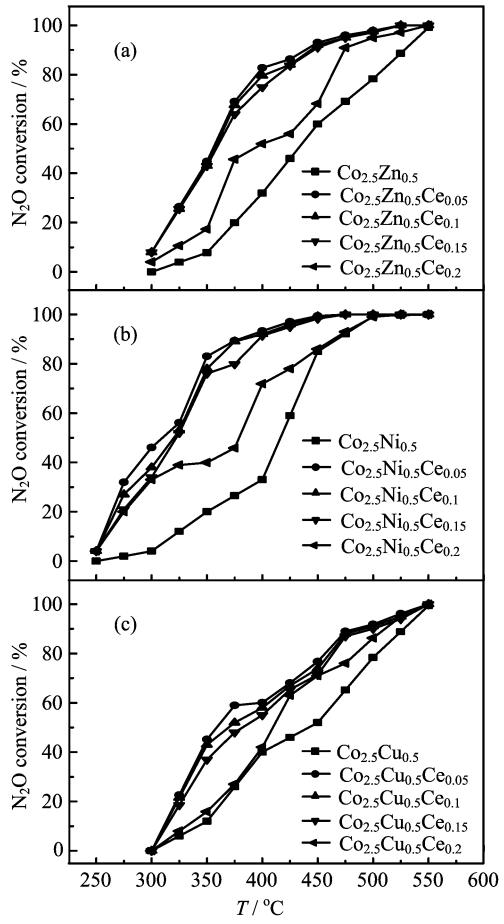


FIG. 4 Conversion of $N_2O$ as a function of reaction temperature over Co-M-Ce-Al mixed oxides. Reaction conditions: 4000 ppm $N_2O$, $N_2$ balance, GHSV=24000 $h^{-1}$.

mixed Ce was 0.05, the catalyst $Co_{2.5}M_{0.5}Ce_{0.05}$ mixed oxide represented the best catalytic activity for $N_2O$ decomposition and the temperatures of 50% and 90% conversion of $N_2O$ ($T_{50}$ and $T_{90}$) were the lowest.

Table I shows the temperatures of 50% and 90% conversion of $N_2O$ ($T_{50}$ and $T_{90}$) over Co-M-Ce-Al mixed oxide catalysts. The temperatures of 50% and 90% conversion of $N_2O$ over $Co_3M_0$ were higher than those of the other catalysts which were partially replaced by $M^{2+}$, indicating that the replacement of $M^{2+}$ improved the catalytic activity. Moreover, compared with $Co_{2.5}Zn_{0.5}$, $T_{50}$ and $T_{90}$ over $Co_{2.5}Zn_{0.5}Ce_{0.05}$ decreased 78 and 91 °C, respectively (shown in Table I), and $T_{50}$ and $T_{90}$ over $Co_{2.5}Ni_{0.5}Ce_{0.05}$ also decreased 107 and 89 °C than those of $Co_{2.5}Ni_{0.5}$, respectively, which was significant in practice. However, $Co_{2.5}Cu_{0.5}Ce_{0.05}$ had the relatively poor catalytic activity, and $T_{50}$ and $T_{90}$ over $Co_{2.5}Cu_{0.5}Ce_{0.05}$ than those of $Co_{2.5}Cu_{0.5}$ decreased 83 and 42 °C, respectively.

In order to inspect the crystal forms and structures of Co-M-Ce-Al hydrotalcite-like catalysts before and after calcining, we chose Co-Ni-Ce-Al-HTLCs and Co-Ni-Ce-Al to be characterized by XRD. From Fig.5(a), we found that the crystallographic indices in XRD patterns of fresh Co-Ni-Ce-Al-HTLCs such as (003), (006), (110), and (113) diffraction lines exhibited the crystal characteristics of hydrotalcite-like materials. With the Ce content increasing, the shape of diffraction peaks became more dispersive and the peak intensity became weaker.

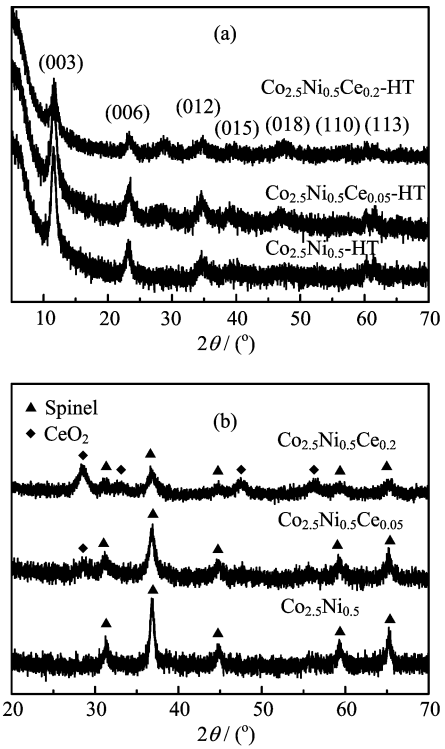


FIG. 5 XRD patterns of (a) Co-Ni-Ce-Al-HTLCs and (b) Co-Ni-Ce-Al mixed oxides.

TABLE I Temperatures of 50% and 90% conversion of $N_2O$ ($T_{50}$ and $T_{90}$) over Co-M-Ce-Al mixed oxide catalysts Catalyst.

| Catalyst | Temperature/°C | |
|---|---|---|
| | $T_{50}$ | $T_{90}$ |
| $Co_3Zn_0$ | 510 | 593 |
| $Co_{2.5}Zn_{0.5}$ | 432 | 529 |
| $Co_{2.5}Zn_{0.5}Ce_{0.05}$ | 354 | 438 |
| $Co_3Ni_0$ | 510 | 593 |
| $Co_{2.5}Ni_{0.5}$ | 417 | 469 |
| $Co_{2.5}Ni_{0.5}Ce_{0.05}$ | 310 | 380 |
| $Co_3Cu_0$ | 510 | 593 |
| $Co_{2.5}Cu_{0.5}$ | 441 | 528 |
| $Co_{2.5}Cu_{0.5}Ce_{0.05}$ | 358 | 486 |

The XRD patterns of calcined Co-Ni-Ce-Al mixed oxides are shown in Fig.5(b). From Fig.5(b), we found the main crystalline phase of $Co_{2.5}Ni_{0.5}$ was spinel phase, while the crystalline phase of $Co_{2.5}Ni_{0.5}Ce_{0.05}$

DOI:10.1063/1674-0068/27/02/233-239 

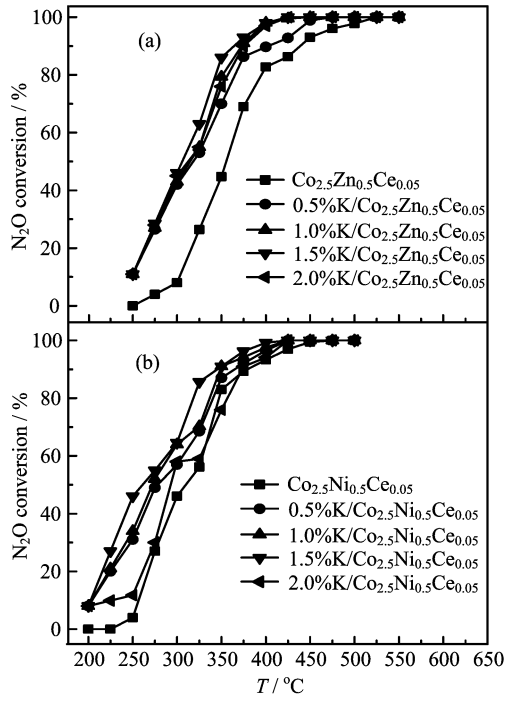


FIG. 6 Conversion of $N_2O$ as a function of reaction temperature over (a) K/Co-Zn-Ce-Al and (b) K/Co-Ni-Ce-Al mixed oxides. Reaction conditions: 4000 ppm $N_2O$, $N_2$ balance, GHSV=24000 $h^{-1}$.

and $Co_{2.5}Ni_{0.5}Ce_{0.2}$ included spinel phase and $CeO_2$ phase, however, the characteristic diffraction peaks of HTLCs disappeared in these samples, indicating the complete collapse of double layered structure after calcination at 500 °C. Compared with $Co_{2.5}Ni_{0.5}Ce_{0.05}$ and $Co_{2.5}Ni_{0.5}Ce_{0.2}$, we found that the diffraction peak of $CeO_2$ phase became increasingly sharp with the Co content increasing, the peak intensity increased, and the crystalline became better, however, the diffraction peak of spinel phase was weaken gradually.

Widmann *et al.* considered $CeO_2$, as one of rare earth materials, was very easy to transform from one to the other because of two kinds of valence states and could be stored and released at the same time to possess special oxidation-reduction properties with excellent reversibility [21]. Hu *et al.* also confirmed the transformation from $Ce^{4+}$ to $Ce^{3+}$ in catalytic desulfurization over rare oxide catalyst [18]. Therefore, we suggested the addition of $CeO_2$ in catalysts led to support more chances for O transference, and it was related to the contribution of oxygen from $CeO_2$ to improve the catalytic activity.

### C. Effect of potassium on catalytic activity of K-Ce promoted Co-M-Al mixed oxides

Figure 6 illustrates the $N_2O$ conversions over Co-Zn/Ni-Ce-Al mixed oxide catalysts modified by loading various amount of potassium. From Fig.6, we found the $K_2CO_3$-doped catalysts were more active than bare Co-Zn/Ni-Ce-Al oxides. With the content increase of potassium loaded, the catalytic activities of the Co-Zn/Ni-Ce-Al mixed oxide catalysts were enhanced significantly until the optimal value of potassium-loaded at 1.5%.

TABLE II Temperatures of 50% and 90% conversion of $N_2O$ ($T_{50}$ and $T_{90}$) over K-Co-Ni-Ce-Al mixed oxide catalysts.

| Catalyst | Temperature/°C | |
|---|---|---|
| | $T_{50}$ | $T_{90}$ |
| $Co_{2.5}Zn_{0.5}Ce_{0.05}$ | 354 | 438 |
| 0.5%K/$Co_{2.5}Zn_{0.5}Ce_{0.05}$ | 319 | 402 |
| 1.0%K/$Co_{2.5}Zn_{0.5}Ce_{0.05}$ | 316 | 373 |
| 1.5%K/$Co_{2.5}Zn_{0.5}Ce_{0.05}$ | 305 | 365 |
| 2.0%K/$Co_{2.5}Zn_{0.5}Ce_{0.05}$ | 312 | 376 |
| $Co_{2.5}Ni_{0.5}Ce_{0.05}$ | 310 | 380 |
| 0.5%K/$Co_{2.5}Ni_{0.5}Ce_{0.05}$ | 278 | 364 |
| 1%K/$Co_{2.5}Ni_{0.5}Ce_{0.05}$ | 272 | 349 |
| 1.5%K/$Co_{2.5}Ni_{0.5}Ce_{0.05}$ | 261 | 346 |
| 2%K/$Co_{2.5}Ni_{0.5}Ce_{0.05}$ | 293 | 372 |

In particular, as shown in Table II, when the mass ratio of $K_2O$ on Co-Zn-Ce-Al mixed oxide was equal to 1.5%, the promotional effect of $K_2O$ was so remarkable that $T_{50}$ and $T_{90}$ were lowered by 49 and 73 °C in comparison with Co-Zn-Ce-Al mixed oxides, and lowered by 127 and 164 °C in comparison with $Co_3O_4$, respectively. While $T_{50}$ and $T_{90}$ over 1.5%K/$Co_{2.5}Ni_{0.5}Ce_{0.05}$Al were 261 and 346 °C, respectively. $T_{50}$ and $T_{90}$ decreased by 49 and 34 °C in comparison with Co-Ni-Ce-Al mixed oxide, and decreased by 156 and 123 °C, in comparison with $Co_3O_4$, respectively. Such a pronounced enhancement was significant for industrialization to decompose $N_2O$ and reduce carbon emission from atmosphere.

The dominant state of surface nickel element was NiO, and from Fig.7(a) we found the peaks of $Ni2p_{1/2}$ and $Ni2p_{3/2}$ of 1.5%K/$Co_{2.5}Ni_{0.5}Ce_{0.05}$ catalyst moved to lower banding energy in comparison with un-promoted catalyst, indicating the weakness of surface Ni−O bond due to the electron donation of K. In Fig.7(b), the peaks of corresponding binding energy (BE) of $Co2p_{3/2}$ and $Co2p_{1/2}$ for 1.5%K/$Co_{2.5}Ni_{0.5}Ce_{0.05}$ were 779.6 and 794.7 eV, respectively. Moreover, the $\Delta E$($Co2p_{1/2}$-$Co2p_{3/2}$) was 15.1 eV. BE of $Co2p_{3/2}$ for 1.5%K/$Co_{2.5}Ni_{0.5}Ce_{0.05}$ decreased 0.3 eV, which was same as that of $Co2p_{1/2}$, in comparison with $Co_{2.5}Ni_{0.5}Ce_{0.05}$, resulting in the further weakness of surface Co−O bond and the desorption of adsorbed oxygen species becoming easier. Eventually the catalytic activity was improved. When potassium was loaded, the banding energy decreased, which indicated the electronic state of Co moved to the lower state. Asano *et al.* suggested that small amount of potassium ions could be adsorbed on the particles to

DOI:10.1063/1674-0068/27/02/233-239 

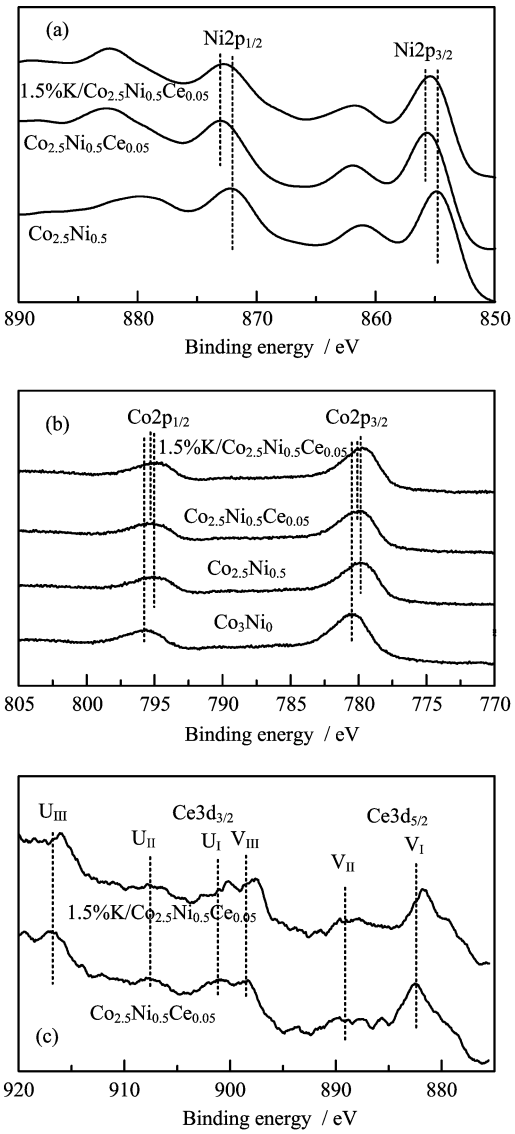


FIG. 7 XPS of (a) Ni2p, (b) Co2p, and (c) Ce3d level for $1.5\%K/Co_{2.5}Ni_{0.5}Ce_{0.05}Al$ mixed oxide.

compensate the negative charge of the particles [22]. Alkali cations were Lewis acids and had no electron donation effects. However, oxygen anions in the coordination sphere of the cations were highly basic and therefore electron donation from highly basic oxygen anions surrounding the alkali cation toward cobalt ion increased the electron density of cobalt ions and played an important role in $N_2O$ decomposition.

Figure 7(c) revealed the XPS of Ce3d level for $Co_{2.5}Ni_{0.5}Ce_{0.05}$ and $1.5\%K/Co_{2.5}Ni_{0.5}Ce_{0.05}$ catalysts, including three patterns for $Ce3d_{5/2}$ ($U_I$, $U_{II}$, $U_{III}$) and three patterns for $Ce3d_{3/2}$ ($V_I$, $V_{II}$, $V_{III}$) [17] to correspond to $Ce^{4+}$, which indicated the loading of alkali metal oxide on $Co_{2.5}Ni_{0.5}Ce_{0.05}$ mixed oxide did not significantly influence the valence state distribution of Ce. From Fig.7(c), we found that the XPS of

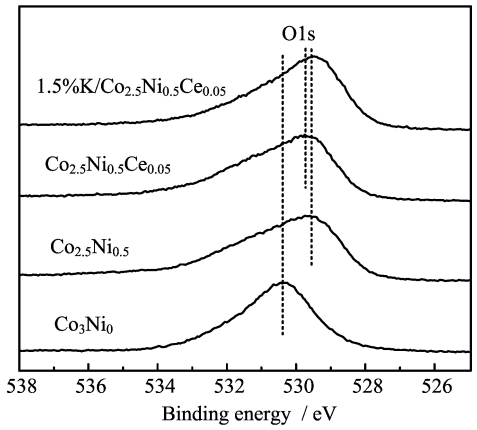


FIG. 8 XPS of O1s level for $1.5\%K/Co_{2.5}Ni_{0.5}Ce_{0.05}Al$ mixed oxide.

Ce3d level for $1.5\%K/Co_{2.5}Ni_{0.5}Ce_{0.05}$ was more intensive than $Co_{2.5}Ni_{0.5}Ce_{0.05}$ and BE of $Ce3d_{5/2}$ and Ce $3d_{3/2}$ were slightly different. It might be one reason for the difference of catalytic activity.

Figure 8 shows the O1s spectra of the catalysts. The peak at 529.0−529.5 eV was attributed to the $O^{2-}$ anions of the crystalline network [23]. The O1s peak slightly shifted toward the lower BE side by the addition of K, indicating that the electronic density of oxygen increased, *i.e.*, the basicity of oxygen anion became high.

## IV. CONCLUSION

Among the Co-M-Al (M=Zn, Ni, Cu) mixed oxide catalysts prepared from hydrotalcite-like precursors with different compositions, the series of $Co_{2.5}M_{0.5}$ mixed oxides showed better catalytic activities. Moreover, the catalytic activity of Co-Ni-Al was slightly higher than that of Co-Zn-Al and much higher than that of Co-Cu-Al in decomposing $N_2O$.

The experiment of Co-M-Ce-Al catalyst for $N_2O$ decomposition indicated $CeO_2$ displayed a key role in improving the catalytic activity and made the decomposition temperatures of both $T_{50}$ and $T_{90}$ decreased 80 °C compared with Co-M-Al catalysts without $CeO_2$ added. Furthermore, the series of $Co_{2.5}M_{0.5}Ce_{0.05}$ mixed oxides had higher catalytic activities.

Potassium-load also had some effect on promoting catalytic activity for direct decomposition of $N_2O$. When the optimal value of potassium-load was 1.5%, the decomposition temperatures $T_{50}$ and $T_{90}$ both decreased approximately 50 °C. It is significant for decomposing $N_2O$ from anthropogenic source such as the nitric acid plant and reducing carbon emission from atmosphere.

DOI:10.1063/1674-0068/27/02/233-239 

## V. ACKNOWLEDGMENTS

This work was supported by the National High-tech R&D Program of China (No.2012AA062501) and the Postgraduates Innovation Foundation of Huazhong University of Science and Technology of China (No.HF-08-11-2011-261). We also thank the analytical support from Analytical and Testing Center of Huazhong University of Science & Technology.

[1] H. P. Wu, W. J. Li, L. Guo, Y. F. Pan, and X. F. Xu, J. Fuel Chem. Technol. **39**, 550 (2011).
[2] G. Centi, L. Dall'Olio, and S. Perathoner, Appl. Catal. A **194**, 79 (2000).
[3] A. R. Ravishankara, J. S. Daniel, and R. W. Portmann, Science **326**, 123 (2009).
[4] F. Kapteijn, J. Rodriguez-Mirasol, and J. Moulijn, Appl. Catal. B **9**, 25 (1996).
[5] A. Shimizu, K. Tanaka, and M. Fujimori, Chemosphere Global Change Sci. **2**, 425 (2000).
[6] M. Odaka, N. Koike, and H. Suzuki, Chemosphere Global Change Sci. **2**, 413 (2000).
[7] L. Yan, T. Ren, X. Wang, D. Ji, and J. Suo, Appl. Catal. B **45**, 85 (2003).
[8] L. Yan, T. Ren, X. Wang, D. Ji, and J. Suo, Catal. Commun. **4**, 505 (2003).
[9] Q. Shen, L. D. Li, J. J. Li, H. Tian, and Z. P. Hao, J. Hazard. Mater. **163**, 1332 (2009).
[10] L. Xue, C. B. Zhang, H. He, and Y. Teraoka, Catal. Today **126**, 449 (2007).
[11] L. Xue and H. He, Acta Phys. Chim. Sin. **23**, 664 (2007).
[12] S. Kannan, Appl. Clay. Sci. **13**, 347 (1998).
[13] Y. X. Tao, J. J. Yu, C. C. Liu, Z. P. Hao, and Z. P. Zhang, Acta Phys. Chim. Sin. **23**, 162 (2007).
[14] H. P. Wu, Z. Y. Qian, X. L. Xu, and X. F. Xu, J. Fuel Chem. Technol. **39**, 115 (2011).
[15] J. J. Yu, L. Zhu, B. Zhou, L. N.Shao, Y. T. Zhang, and X. W. He, Acta Phys. Chim. Sin. **25**, 353 (2009).
[16] K. Karásková, L. Obalová, K. Jirátová, and F. Kovanda, Chem. Eng. J. **160**, 480 (2010).
[17] L. Xue, C. B. Zhang, H. He, and Y. Teraoka, Appl. Catal. B **75**, 167 (2007).
[18] H. Hu, S. L. Li, S. X. Zhang, and J. Li, Chin. J. Catal. **25**, 115 (2004).
[19] S. Kannan and C. S. Swamy, Catal. Today **53**, 725 (1999).
[20] J. M.Fernández, M. A. Ulibarri, F. M. Labajos, and V. Rives, J. Mater. Chem. **8**, 2507 (1998).
[21] D. Widmann, R. Leppelt, and R. J. Behm, J. Catal. **251**, 437 (2007).
[22] K. Asano, C. Ohnishi, S. Iwamoto, Y. Shioya, and M. Inoue, Appl. Catal. B **78**, 242 (2008).
[23] A. Miyakoshi, A. Ueno, and M. Ichikawa, Appl. Catal. A **219**, 249 (2001).

DOI:10.1063/1674-0068/27/02/233-239 